Cascade attitude control of a quadcopter in presence of motor asymmetry ⋆

Brice J. Njinwoua * **Alain Vande Wouwer.** *

* *University of Mons - Control Department, 7000 Mons, Belgium.*

Abstract: The quadcopter is one of the most used unmanned aerial vehicles in both military and commercial in- and outdoor applications. In this study, the problem of UAV attitude control is investigated when there are discrepancies in the characteristics of the 4 actuators, i.e., electrical motors and propellers. To tackle this problem in a simple way, a cascade control strategy is proposed with a PD controller in the inner loop to achieve stabilization, and PI controller in the outer loop to ensure disturbance rejection. This way, the external disturbance created by the actuator asymmetry is compensated by the PI loop. The robustness of the control strategy is tested in simulation as well as in real-life tests on a 1-DOF test bed.

Keywords: Unmanned Aerial Vehicles, PID control, Disturbance rejection.

1. INTRODUCTION

Unmanned Aerial Vehicles, known as UAVs, have known a growing interest in the last decade. This increasing popularity is due to their low cost, simple construction, manoeuvrability and stability (Abas et al., 2013). They are used in a vast array of applications, including military applications (rescue, border surveillance), industry and agriculture applications (pipe maintenance, field monitoring), movie production, logistics, and leisure. UAVs can be classified in two categories : aeroplane and multirotors. Multirotors have advantages in terms of manoeuvrability in limited space and better hovering operation (Barve and Patel, 2014).

Different multirotor configurations are available, and in this study, a quadcopter (or quadrotor) is under consideration. A quadcopter has 6 degrees of freedom(3 linear and 3 angular positions) and is controlled by 4 motors.

In this connection, the first research topics focused on dynamic modelling of the copter (Hoffmann et al., 2007) followed by the introduction of more complex aero-dynamical effects (Huang et al., 2009). Several control strategies were then designed, starting from basic PID controllers (Dikmen et al., 2009; Bolandi et al., 2013), and proceeding with LQR controllers (Bouabdallah et al., 2004), Feedback control based on the representation in quaternions (Fresk and Nikolakopoulos, 2013), back-stepping control (Madani and Benallegue, 2006; Bouabdallah and Siegwart, 2005), H_∞ control (Raffo et al., 2010), feedback linearisation (Benallegue et al., 2006) and cascade control Achtelik et al. (2011); Szafranski and Czyba (2011); Tesch et al. (2016). Since control strategies require measurements of the position and the attitude of the copter, several techniques were also developed to estimate accurately this information. The estimators used for UAVs are Kalman filtering (KF) and the complementary filter (CF) (Martin and Salaün, 2010). Extended Kalman Filters (EKF) and Unscented Kalman Filters (UKF) were also considered (Abas et al., 2013), but CF is usually the preferred solution because of its simplicity and high efficiency (Chang-Siu et al., 2011).

In several cases, control strategies such as PID are based on several simplifying assumptions. One of those is to assume that the actuators are identical. However, this is not always verified in practice, and can considerably affect the controller performance. To take the uncertainties into account, some researchers have designed advanced control strategies, such as switching MPC (Alexis et al., 2011), integral back-stepping control (Bouabdallah and Siegwart, 2007), adaptive PID control (Fatan et al., 2013), etc.

In this work, a simple control strategy is proposed, that is easy to implement and fully functional on a basic 16 MHz chip. This control strategy is a cascade control with a PD controller in the inner loop to achieve stabilization, and a PI control in the outer loop to achieve performance (disturbance rejection).

This paper is organized as follows : Section 2 presents the dynamical model of the quadcopter and some experimental results allowing parameter calibration. In Section 3, the characteristics of the actuators are discussed and the cascade control structure is developed. The simulation and experimental results are presented and discussed in Section 4. Conclusions are drawn in Section 5.

2. DYNAMIC MODEL

2.1 Description

A quadcopter is a flying object carried by four parallel propellers mounted on two pairs of counter rotating motors. It has six degrees of freedom in the inertial frame, with variables x, y, z, U, V, W (linear positions and velocities), ϕ, θ, ψ, P, Q, R (angular positions and velocities) as shown on Fig. 1. The rotation around the x, y and z axis are respectively called $Roll$, $Pitch$ and Yaw.
The rotation of the propellers creates two effects: a thrust or lift force and a drag torque. By varying the motor speed,

⋆ University of Mons, Mons, Belgium (e-mail : Alain.Vandewouwer@umons.ac.be).

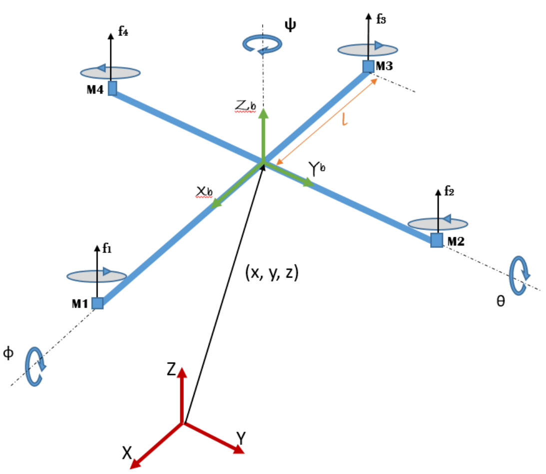

Fig. 1. Quadcopter coordinate system.

several motion types can be generated. To increase the pitch, the speeds of motor 3 and 1 have to be increased and decreased, respectively (or vice versa to decrease the pitch). The roll can similarly be manipulated by acting on motors 2 and 4. For spinning around the z-axis in a given direction, the speed of the motors rotating in the chosen direction has to be increased, while the speed of the counter-rotating motors has to be decreased in opposite direction.

2.2 Dynamic modelling

The lift force f_i generated by the rotation of the propeller i is calculated as (Barve and Patel, 2014):

$$f_i = \rho(H) C_T A R^2 \omega_i^2 \simeq k_t \omega_i^2 \quad (1)$$

where C_T is the thrust coefficient, ρ is the air density (function of the elevation), A is the rotor disk area and R is the blade radius.

The drag torque τ_i is given by (Barve and Patel, 2014):

$$\tau_i = k_d \omega_i^2 \quad (2)$$

where k_d is the drag coefficient of the propeller.

The forces and torques acting on the copter can thus be computed as :

$$\begin{aligned} U_H &= k_t(\omega_1^2 + \omega_2^2 + \omega_3^2 + \omega_4^2) \\ U_\phi &= l k_t(\omega_2^2 - \omega_4^2) \\ U_\theta &= l k_t(\omega_3^2 - \omega_1^2) \\ U_\psi &= k_d(\omega_1^2 - \omega_2^2 + \omega_3^2 - \omega_4^2) \end{aligned} \quad (3)$$

where U_H, U_ϕ, U_θ and U_ψ are the control inputs representative of the total trust, roll, pitch and yaw torque respectively and l the distance from the centre of the copter to the centre of the rotors. In this study, we consider a hovering flight with small variations of the angles to achieve copter stabilization, and a simplified linear model can be considered to design the control strategy. The (simplified) dynamics can be derived using Newton second law and a transformation matrix (Barve and Patel, 2014).

$$\begin{aligned} \ddot{x} &= U_H(\sin\psi \sin\phi + \cos\psi \sin\theta \cos\phi)/m \\ \ddot{y} &= U_H(\sin\psi \sin\theta \cos\phi - \cos\psi \sin\phi)/m \\ \ddot{z} &= U_H \cos\phi \cos\theta/m - g \\ \ddot{\phi} &= U_\phi/I_{xx} \\ \ddot{\theta} &= U_\theta/I_{yy} \\ \ddot{\psi} &= U_\psi/I_{zz} \end{aligned} \quad (4)$$

where I_{xx}, I_{yy}, I_{zz} are the rotary inertia around **x**, **y** and **z** and and m the total mass of the quadcopter, respectively.

The selected frame is the famous DJI F450 and the control unit is a *Arduino UNO* running at $16 Mhz$ with a 8-bit micro-controller. The Electronic Speed Controller (ESC) is 420 Lite 4S 20A, which controls the four DJI motors 2312 E 960KV. Experiments following the protocol described in (Mustapha et al., 2014) were achieved to determine the values of k_t and k_d. The inertia I_{xx}, I_{yy} and I_{zz} were calculated by representing the quadcopter by separate simple components idealized with simple geometric shapes, such as cylinders, flat plates and rectangular parallelepipeds, in order to enable the use of classic formulas. The resulting inertia around the copter axes were then determined using the parallel-axis theorem and summed to obtain the global contribution [(Jones, 1975)]. The parameters are listed in Table 1.

Table 1. Copter parameters

Parameter	Value	Description
m	1.15kg	Total mass
l	16cm	Dist. center-motors
I_{xx}	$127.5\text{kg} \cdot \text{cm}^2$	Inertia abt x-axis
I_{yy}	$127.5\text{kg} \cdot \text{cm}^2$	Inertia abt y-axis
I_{zz}	$242.3\text{kg} \cdot \text{m}^2$	Inertia abt z-axis
k_t	$8.2 \times 10^{-5} N \cdot s^2/rad^2$	Thrust factor
k_d	$1.52 \times 10^{-7} N \cdot m \cdot s^2/rad^2$	Drag factor

3. PROBLEM STATEMENT AND CONTROLLER DESIGN

The control objective is to set the attitude angles ϕ, θ and ψ to stabilize the copter, despite discrepancies in the motors characteristics and propellers geometry.

For the sake of simplicity, only the control design for the roll angle ϕ is described, but the same approach can be applied for the pitch and yaw angles.

Lemma 1. In case of actuators (rotor + propeller) asymmetry, the thrust and drag coefficients can differ from motor to motor. The resulting effect is a disturbance proportional to the difference δk_t in the coefficients of the considered actuators.

Proof. Eq. (4) and (3) give :

$$\begin{aligned} I_{xx}\ddot{\phi} &= U_\phi \\ &= l(k_{t_2}\omega_2^2 - k_{t_4}\omega_4^2) \end{aligned} \quad (5)$$

If we consider an equilibrium point, where $\omega_2 = \omega_4 = \omega_0$, and a small variation $\delta\omega$ of the angular velocity, the linearised model is given by:

$$\begin{aligned} \frac{I_{xx}}{l}\ddot{\phi} &= 2k_{t_2}(\omega_0 + \delta\omega) - 2k_{t_4}(\omega_0 - \delta\omega) \\ &= 2\omega_0(k_{t_2} - k_{t_4}) + 2\delta\omega(k_{t_2} + k_{t_4}) \end{aligned} \quad (6)$$

If $k_{t_2} \neq k_{t_4}$, there is a disturbance $P = 2\omega_0(k_{t_2} - k_{t_4})$.

Several experiments have been carried out to assess the characteristics of the actuators. Since the motors are controlled with a servo signal, the speed is modified by changing the duty cycle through the pulse length (1100 - 1900μs). The characteristics of actuator 2 and 4 are shown in figure 2.

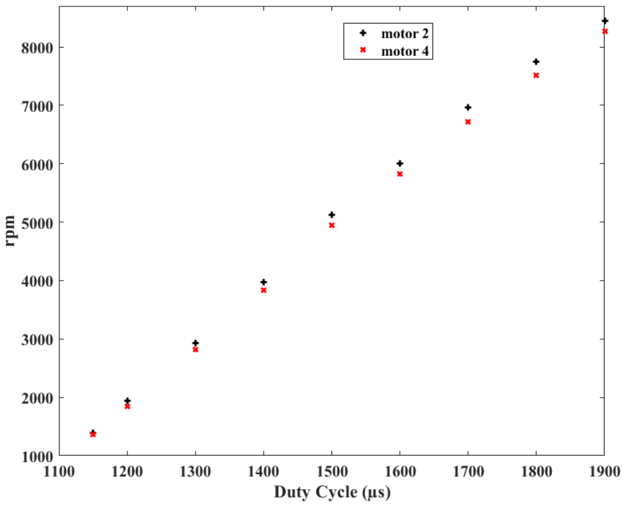

Fig. 2. Motor characteristics.

The open-loop system is represented in figure 3.

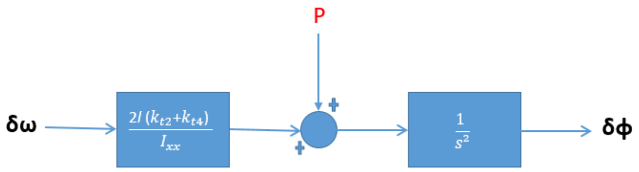

Fig. 3. Open-loop system with disturbance.

To compensate the disturbance action, we need a controller with an integrator before the disturbance.

A cascade control structure is proposed with a PD controller in the inner loop for system stabilization, and a PI controller in the outer loop for disturbance rejection.

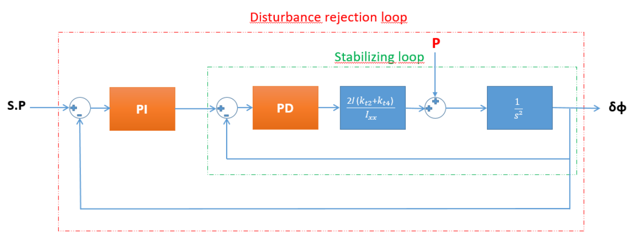

Fig. 4. Cascade control.

Tuning of the controllers : The stabilizing loop is first closed and the PD controller is tuned to guarantee quick response with no steady state error when there is no disturbance. The second loop is then closed and the disturbance is added before the tuning of the PI controller. The discrete controllers have the following structure :

$$C_{PID} = P + I \cdot T_s \frac{1}{z-1} + D \frac{1}{T_s} \frac{z-1}{z} \tag{7}$$

The controllers were tuned using the Matlab PID Tool Box to guarantee stability, robustness and fast dynamics in closed-loop. The sampling period T_s was chosen to compromise speed of reaction and computational load of the micro-controller. The values are listed in table 2.

Table 2. Parameters of the controllers.

Controller	P	I	D	T_s
PD	2.95	-	2.6	$4\ ms$
PI	1.8	3.75	-	$4\ ms$

Actuator saturation has to be considered - the physical limits of the ESC are $1100 - 1900\mu s$ - and an anti-reset wind-up using Back-calculation scheme is added with a tracking time constant $K_b = 2.75$ found experimentally by following the guidelines described in [(Astrom, 2002)].

4. RESULTS AND DISCUSSIONS

4.1 Simulation results

Simulation tests of the roll control loop are achieved with the other loops open. Initial conditions of 0.1, -0.1 and 0 for the roll, pitch and yaw angles, respectively, are used and the pulse length of the four motors is taken equal to 1500μs. The results with asymmetry (10%) and without are presented in figures 5

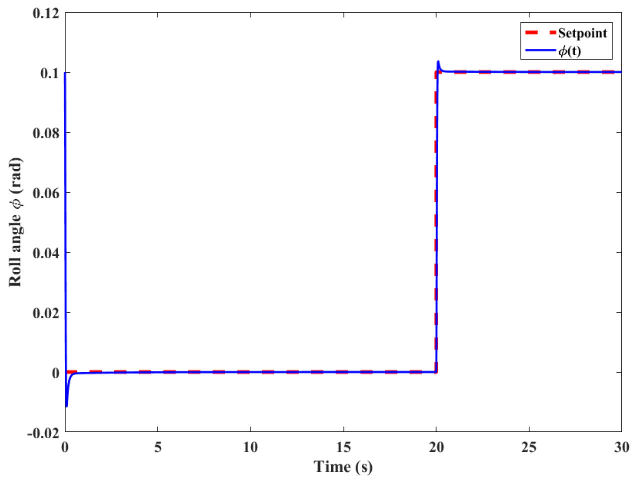

Fig. 5. Time evolution of the roll angle with no asymmetry.

The results of the roll, pitch and yaw angles in the global closed-loop system are shown in Fig. 9, 10 and 11 respectively.

4.2 Discussions

At first, we look at the individual loops to avoid disturbances created by coupling effects. As we can see in Fig. 5, the controller performs well when the actuators are exactly the same (no asymmetry). The overshoot is less than 5%

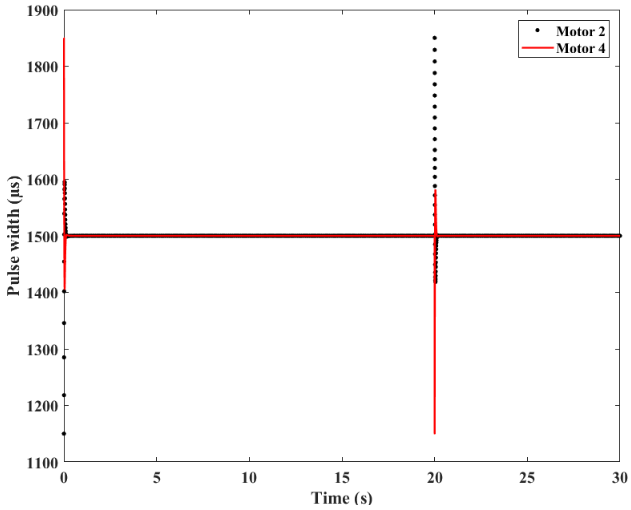

Fig. 6. Time evolution of the input signal with no asymmetry.

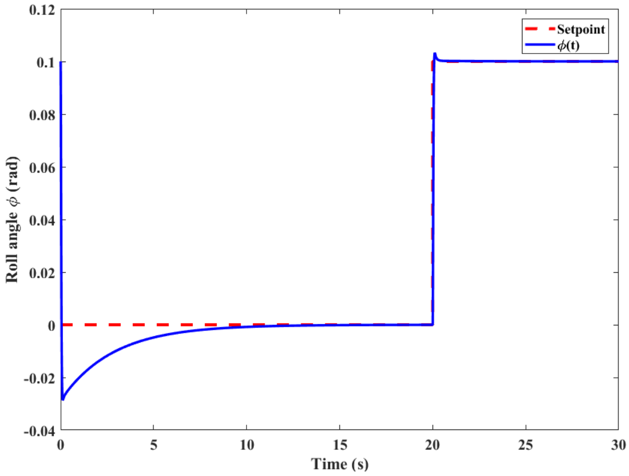

Fig. 7. Time evolution of the roll angle with 10% asymmetry.

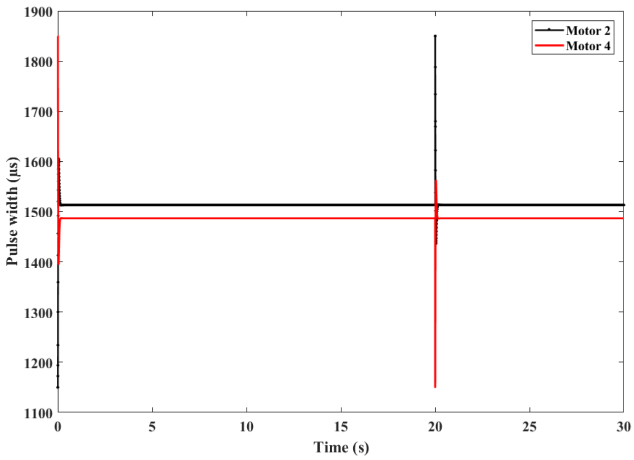

Fig. 8. Time evolution of the input signal with 10% asymmetry.

and the settling time is about $1s$. The control inputs (see Fig. 6) at steady state are the initial values ($1500\mu s$) as there is no disturbance to compensate.
When an asymmetry of 10% is considered, the overshoot

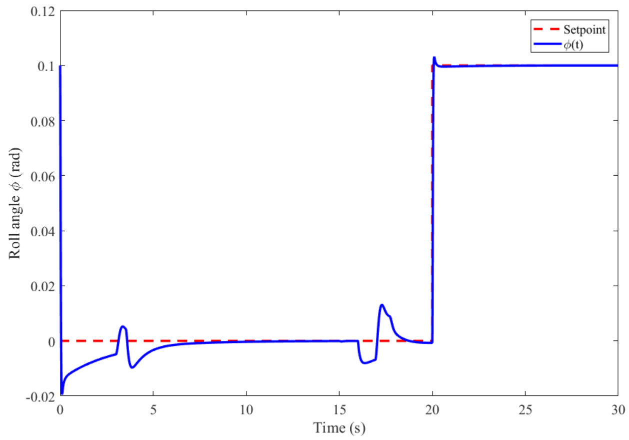

Fig. 9. Roll angle : closed-loop system.

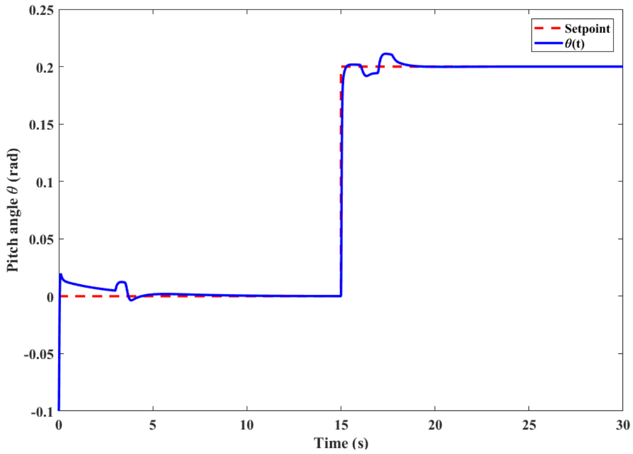

Fig. 10. Pitch angle.

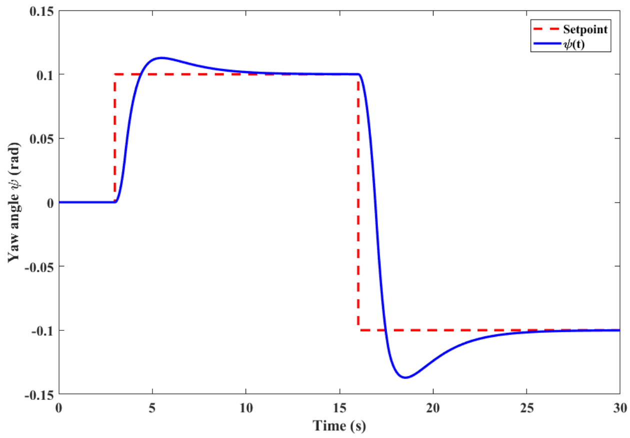

Fig. 11. Yaw angle.

increases as well as the settling time, which is now at around $7s$ for the first control objective (Fig. 7). At steady state, the motor inputs are different enough to generated the same lift effect (Fig. 8). Once the equilibrium point is reached, the tracking performances are similar to the case without discrepancies (See Fig. 7 second control objective at $20s$).
By closing all the control loops, the coupling action between the yaw, pitch and roll appears. This can be seen as a second disturbance in addition to the deviations in

the drag and lift factors of each actuator. As the yaw angle is less important than the roll and pitch angles for stabilisation, the closed-loop dynamics is chosen slower than the ones of the other loops (Fig. 11). The overshoot is about 10% and the settling time $5s$ with 5% asymmetry on the lift and drag factors.
The controllers on the roll and pitch angles compensate quickly ($3s$) the disturbance introduced by the set-point change on the yaw angle (see Fig. 9 and 10).

4.3 Experimental results

The control law was implemented on an Arduino Uno clocked with a 8-bit $16Mhz$-micro-controller, with a sampling time of $4ms$. Attitude measurement was obtained using a complementary filter combining data from the accelerometer and the gyroscope of IMU 6050.

The copter was mounted on a 1-DOF bench test, as shown in Fig. 12 to control the roll angle. We assume that the effect of the shaft's inertia are small, thus can be neglected. Results are shown in Fig. 13.

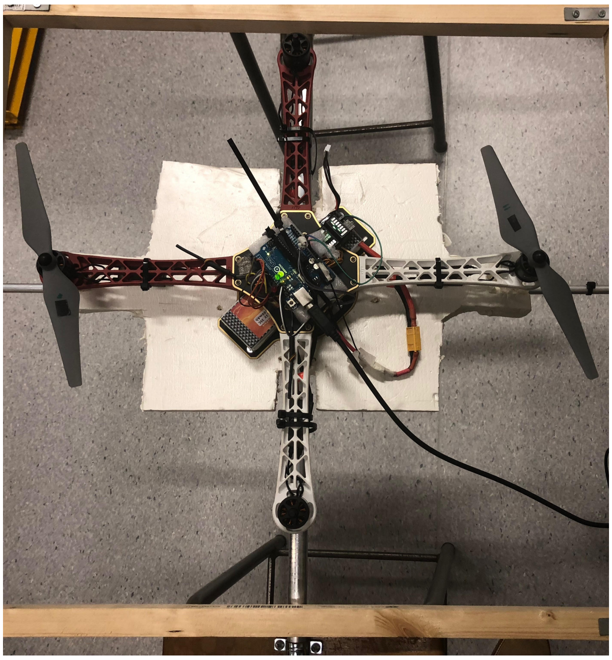

Fig. 12. The 1-DOF test platform.

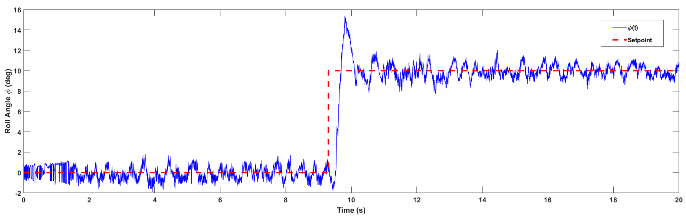

Fig. 13. Roll angle control.

The controller performs well, although the bench creates an extra disturbance due to its geometrical asymmetry, its extra inertia and the recirculating airflow created by the propellers and the ground. The oscillations are due to the noisy measurements which can be attenuated using a Kalman filter.

5. CONCLUSION

Asymmetry in the actuators of UAVs is frequent, and create external disturbances that need to be compensated by feedback control. In this study, a simple control strategy based on a PD controller in the inner loop and a PI controller in the outer loop is proposed and tested in simulation and experiments. The present study assumes small deviations, and a simplified dynamic model. Future work entails the study of larger moves and the effect of nonlinearities.

REFERENCES

Abas, N., Legowo, A., Ibrahim, Z., Rahim, N., and Kassim, A.M. (2013). Modeling and system identification using extended kalman filter for a quadrotor system. In *Applied Mechanics and Materials*, volume 313, 976–981. Trans Tech Publ.

Achtelik, M., Bierling, T., Wang, J., Hocht, L., and Holzapfel, F. (2011). Adaptive control of a quadcopter in the presence of large/complete parameter uncertainties. *Infotech@ Aerospace*, 29–31.

Alexis, K., Nikolakopoulos, G., and Tzes, A. (2011). Switching model predictive attitude control for a quadrotor helicopter subject to atmospheric disturbances. *Control Engineering Practice*, 19(10), 1195–1207.

Astrom, K.J. (2002). Pid control. In *Control System Design*, 216–251.

Barve, J. and Patel, K. (2014). Modelling, simulation and altitude-range-analysis of quad-copter uav. *IFAC Proceedings Volumes*, 47(1), 1126–1130.

Benallegue, A., Mokhtari, A., and Fridman, L. (2006). Feedback linearization and high order sliding mode observer for a quadrotor uav. In *Variable Structure Systems, 2006. VSS'06. International Workshop on*, 365–372. IEEE.

Bolandi, H., Rezaei, M., Mohsenipour, R., Nemati, H., and Smailzadeh, S.M. (2013). Attitude control of a quadrotor with optimized pid controller. *Intelligent Control and Automation*, 4(03), 335.

Bouabdallah, S., Noth, A., and Siegwart, R. (2004). Pid vs lq control techniques applied to an indoor micro quadrotor. In *Intelligent Robots and Systems, 2004.(IROS 2004). Proceedings. 2004 IEEE/RSJ International Conference on*, volume 3, 2451–2456. IEEE.

Bouabdallah, S. and Siegwart, R. (2005). Backstepping and sliding-mode techniques applied to an indoor micro quadrotor. In *Robotics and Automation, 2005. ICRA 2005. Proceedings of the 2005 IEEE International Conference on*, 2247–2252. IEEE.

Bouabdallah, S. and Siegwart, R. (2007). Full control of a quadrotor. In *Intelligent robots and systems, 2007. IROS 2007. IEEE/RSJ international conference on*, 153–158. Ieee.

Chang-Siu, E., Tomizuka, M., and Kong, K. (2011). Time-varying complementary filtering for attitude estimation. In *Intelligent Robots and Systems (IROS), 2011 IEEE/RSJ International Conference on*, 2474–2480. IEEE.

Dikmen, I.C., Arisoy, A., and Temeltas, H. (2009). Attitude control of a quadrotor. In *Recent Advances in*

Space Technologies, 2009. RAST'09. 4th International Conference on, 722–727. IEEE.

Fatan, M., Sefidgari, B.L., and Barenji, A.V. (2013). An adaptive neuro pid for controlling the altitude of quadcopter robot. In *Methods and models in automation and robotics (mmar), 2013 18th international conference on*, 662–665. IEEE.

Fresk, E. and Nikolakopoulos, G. (2013). Full quaternion based attitude control for a quadrotor. In *Control Conference (ECC), 2013 European*, 3864–3869. IEEE.

Hoffmann, G.M., Huang, H., Waslander, S.L., and Tomlin, C.J. (2007). Quadrotor helicopter flight dynamics and control: Theory and experiment. In *Proc. of the AIAA Guidance, Navigation, and Control Conference*, volume 2, 4.

Huang, H., Hoffmann, G.M., Waslander, S.L., and Tomlin, C.J. (2009). Aerodynamics and control of autonomous quadrotor helicopters in aggressive maneuvering. In *Robotics and Automation, 2009. ICRA'09. IEEE International Conference on*, 3277–3282. IEEE.

Jones, R.M. (1975). *Mechanics of composite materials*, volume 193. Scripta Book Company Washington, DC.

Madani, T. and Benallegue, A. (2006). Backstepping control for a quadrotor helicopter. In *Intelligent Robots and Systems, 2006 IEEE/RSJ International Conference on*, 3255–3260. IEEE.

Martin, P. and Salaün, E. (2010). The true role of accelerometer feedback in quadrotor control. In *Robotics and Automation (ICRA), 2010 IEEE International Conference on*, 1623–1629. IEEE.

Mustapha, Z., Saat, S., Husin, S., and Zaid, T. (2014). Quadcopter physical parameter identification and altitude system analysis. In *Industrial Electronics & Applications (ISIEA), 2014 IEEE Symposium on*, 130–135. IEEE.

Raffo, G.V., Ortega, M.G., and Rubio, F.R. (2010). An integral predictive/nonlinear h control structure for a quadrotor helicopter. *Automatica*, 46(1), 29–39.

Szafranski, G. and Czyba, R. (2011). Different approaches of pid control uav type quadrotor.

Tesch, D.A., Eckhard, D., and Guarienti, W.C. (2016). Pitch and roll control of a quadcopter using cascade iterative feedback tuning. *IFAC-PapersOnLine*, 49(30), 30 – 35. doi:https://doi.org/10.1016/j.ifacol.2016.11.118. 4th IFAC Symposium on Telematics Applications TA 2016.